

MODELLING AND STATIC ANALYSIS OF TWO DIMENSIONAL REGIONS CONTAINING MULTI-PHASE INCLUSIONS BY BOUNDARY ELEMENT METHOD

SONIA PARVANOVA

*University of Architecture, Civil Engineering and Geodesy,
1, Christo Smirnenski Blvd, 1046 Sofia, Bulgaria,
e-mail: slp_fce@uacg.bg*

[Received 15 February 2010. Accepted 04 October 2010]

ABSTRACT. In this paper an idea related to the effective implementation of the Boundary Element Method (BEM) is developed. This procedure is very suitable for modelling a composite medium with large number of identical inclusions, because its application results to considerable reduction of the model's degrees of freedom. This reduction is proportional to the number of inclusion phases: larger number of phases smaller degrees of freedom compared to classical BEM modelling. A recurrent formula for excluding the inside inclusion nodal values is derived and used in the computer code. It turns out that the elaborated technique can be applied for the static micromechanical analysis of composites containing repeated geometric structures representing openings, cracks or multiphase inclusions uniformly or randomly distributed in the matrix. One numerical example is presented along with some numerical results. They are compared with the results based on the finite element method solution, performed by the well known ANSYS general purpose program.

KEY WORDS: boundary element method, effective solution, 2D theory of elasticity, composite medium.

1. Introduction

The composites are widely used recently in many engineering applications. For that reason the micro- and macro- mechanical behaviour of such materials has been studied by the researchers [1–7]. One of the objects of micro-mechanics is the prediction of macroscopic modulus of heterogeneous materials when the elastic properties of their individual phases are given [2]. In most cases such investigations are carried out by the application of Finite Element Method (FEM) [2, 3]. In FEM numerical models very fine meshes need to be

applied inside and around the inter-phase layers which results in large number of degrees of freedom. In these models the concept of repeating unit cell with a regular distribution of inclusions is usually employed. Even though, the method is computationally sensitive and the accuracy depends on the mesh size. The boundary element method is a powerful competitor of the most universal finite element method in many problems [4–7]. The main advantages of BEM are the high accuracy due to the using of fundamental solutions and the reduction of the dimensionality of the problem. A substantial limitation of the conventional BEM, in modelling the composite mediums, comes from the drawback of the collocation method which puts some restrictions on the thickness of the different phases.

An idea related to the effective implementation of the BEM is developed in the present paper. The proposed procedure leads to reduction of the number of degrees of freedom of BEM models compared to the conventional application of the method. A similar idea in the case of two phase inclusions has been developed in paper [6]. The numerical technique is very suitable for micromechanical analysis of composites containing identical inclusions uniformly or randomly distributed in the matrix. The effectiveness of the developed procedure arises with the increasing of the number of inclusion phases. In accordance with this procedure the basic unknowns of the BEM model are the unknown boundary values of the outside contour and the displacements of the last outer inclusion boundary. The displacements and tractions discrete values of an arbitrary inside inclusion contour can be defined by a simple recurrent formula derived in the paper. In that respect, once the basic unknowns are calculated all nodal values of the inside boundaries can be found.

2. Formulation of the boundary element method

The displacement boundary integral equation is generally used as a starting point for the boundary elements. This equation is worked out in [8, 9], for a domain with a smooth contour Γ , and can be presented by the following expression:

$$(1) \quad \frac{1}{2}u_j(x_0) = \int_{\Gamma} u_{ij}^*(x_0, x)t_i(x)d\Gamma(x) - \int_{\Gamma} t_{ij}^*(x_0, x)u_i(x)d\Gamma(x).$$

In equation (1) the indices i and j range from 1 to 2 and refer to the Cartesian coordinate directions; $u_j(x)$ and $t_j(x)$ are displacement and traction functions on the boundary Γ respectively; u_{ij}^* and t_{ij}^* represent the Kelvin's displacement and traction fundamental solutions at a boundary point x .

The numerical solution of the system of linear algebraic equations requires dividing of the contours with boundary elements. The type of elements can be chosen from constant, linear, quadratic or higher order elements depending on the problem to be solved. The constant or linear elements are appropriate for plane elasticity problems. Also, boundary elements can be continuous or discontinuous depending on the location of the nodes. A non-linear variant of the dual boundary element method has been developed in paper [9] and applied using a discontinuous double-node linear boundary element for 2D plane elasticity crack problems. Here, the same program code is used to which an extension is made for modelling the composite medium. The point is that in the future closed cohesive cracks can be involved in the composite modelling. That is why in the present study the discontinuous boundary element is used although the problem in hand can be successfully solved by continuous boundary elements.

The displacement boundary integral equation written in discrete form reads [9]:

$$(2) \quad \frac{1}{2} \mathbf{u} = \sum_{k=1}^n \underbrace{\left(\int_{\Gamma_k} \mathbf{u}^* \Phi^T d\Gamma \right)}_{\mathbf{G}^k} \mathbf{t}^k - \sum_{k=1}^n \underbrace{\left(\int_{\Gamma_k} \mathbf{t}^* \Phi^T d\Gamma \right)}_{\mathbf{H}^k} \mathbf{u}^k = \sum_{k=1}^n \mathbf{G}^k \mathbf{t}^k - \sum_{k=1}^n \mathbf{H}^k \mathbf{u}^k.$$

The sum is over the boundary elements and the matrices \mathbf{G}^k and \mathbf{H}^k are related to the k -th element in equation (2) and contain integrals of the fundamental solutions (\mathbf{u}^* , \mathbf{t}^*) and shape functions Φ .

The integration over the boundary elements, in the above expressions, has been computed numerically using Gauss quadratic formula. The numerical integration cannot be applied when the collocation point is a node of the element into consideration, because the fundamental solutions are singular. In this case, the singular integrals have been solved analytically [9].

Taking each nodal point in turn as the collocation point, the boundary integral equation is transformed into the following matrix system of equations:

$$(3) \quad \mathbf{G} \cdot \mathbf{t} - \mathbf{H} \cdot \mathbf{u} = \mathbf{0}.$$

Matrices \mathbf{G} and \mathbf{H} are the final influence matrices. They are full matrices of size $4N/4N$ where N is the number of the boundary elements. The global vectors \mathbf{u} and \mathbf{t} of size $4N$ contain the boundary displacement and traction components respectively.

3. Modelling of the regions containing inclusions with different material phases. Description of the standard BEM procedure

Normally, the composites consist of basic continuous material, called matrix, and a number of elastic inclusions as shown in Fig. 1. In most cases, all inclusions have identical dimensions and shape but different elastic characteristics from the matrix. The mechanical properties of the different phases are known in advance.

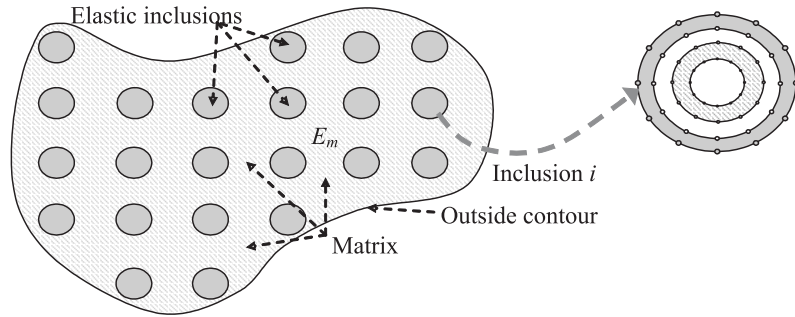


Fig. 1. A composite domain made of matrix with elastic modulus E_m and a system of elastic inclusions of different phases

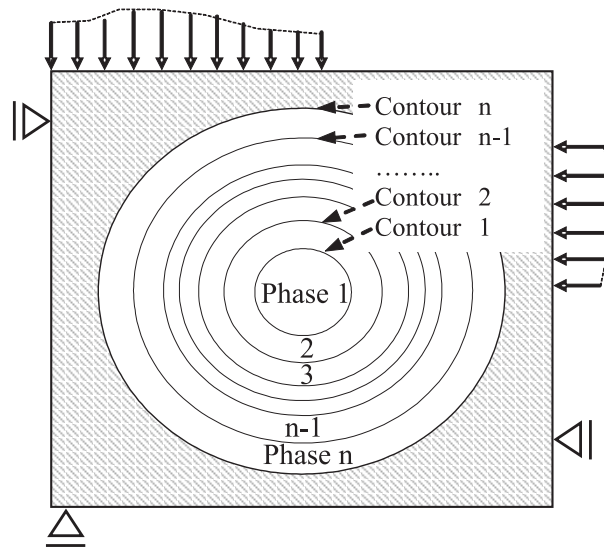


Fig. 2. A rectangular domain containing single inclusion with n different phases

A rectangular matrix domain with a single inclusion is shown in Fig. 2. The inclusions are generally arbitrary shaped, located randomly in the matrix domain. In the numerical simulations however, they are usually modelled as circles periodically distributed in the matrix region. The shape of the outside contour can be arbitrary, but the usual form for plane elasticity problems is a rectangular one. The inclusion under consideration consists of n different phases respectively each phase has unique mechanical properties. At each nodal point according to the basic idea of BEM two discrete values of the displacements and two discrete values of the tractions are available. Two of the discrete values for outside matrix contour are known from the boundary conditions, whereas for each of the inclusion contours all discrete values are unknown. The following system of linear equations considering the matrix domain presented in Fig. 3(a), which includes outside boundary referred to as m and the inclusion contour of the last phase n , could be generated:

$$(4) \quad \mathbf{G}^m \cdot \mathbf{t}^m - \mathbf{H}^m \cdot \mathbf{u}^m = \mathbf{0}.$$

The boundary element discrete model of the domain into consideration is shown in Fig. 3(a).

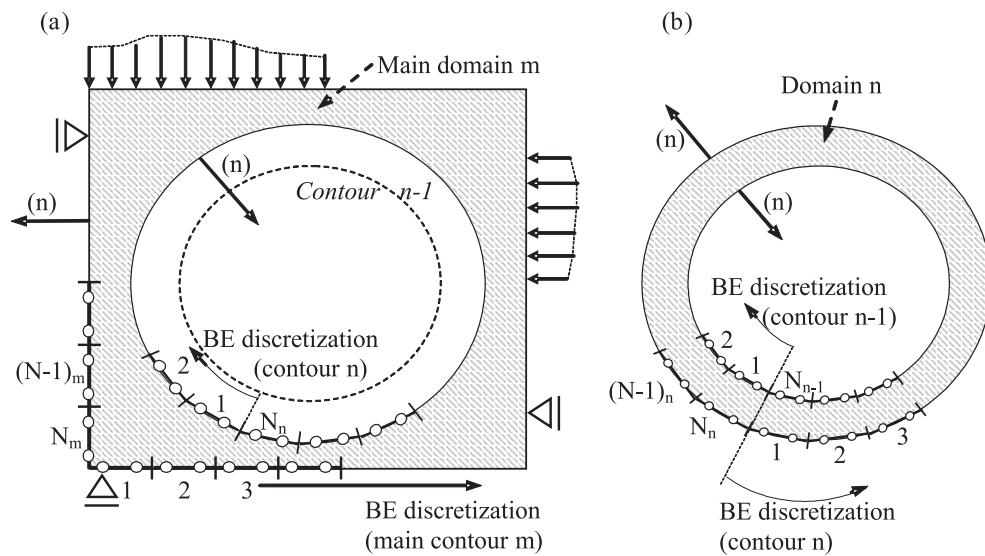


Fig. 3. BE models: (a) matrix domain; (b) last phase of the inclusion

The system of equations (4) can be presented in an expanded form as follows:

$$(5) \quad \begin{bmatrix} \mathbf{G}_{m,m}^m & \mathbf{G}_{m,n}^m \\ \mathbf{G}_{n,m}^m & \mathbf{G}_{n,n}^m \end{bmatrix} \begin{Bmatrix} \mathbf{t}_m^m \\ \mathbf{t}_n^m \end{Bmatrix} = \begin{bmatrix} \mathbf{H}_{m,m}^m & \mathbf{H}_{m,n}^m \\ \mathbf{H}_{n,m}^m & \mathbf{H}_{n,n}^m \end{bmatrix} \begin{Bmatrix} \mathbf{u}_m^m \\ \mathbf{u}_n^m \end{Bmatrix}.$$

Values \mathbf{G}^m and \mathbf{H}^m in equations (4) are global influence matrices for the model into consideration with respect to the matrix domain denoted as m . They are compounded of sub-matrices as shown in formula (5): $\mathbf{G}_{m,m}^m$ is the matrix of the basic contour influenced by the same contour quantities, $\mathbf{G}_{m,n}^m$ is the outside boundary matrix influenced by the last inclusion contour, likewise $\mathbf{G}_{n,m}^m$ is the inclusion matrix influenced by the basic contour and finally $\mathbf{G}_{n,n}^m$ is again the final inclusion phase matrix but influenced by the same inclusion contour. Elsewhere in this paper the superscript notation indicates the region into consideration. The subscript notations show the respective contour; correspondingly the first one indicates the source point contour, whereas the second one is the contour of the field point. In that respect, \mathbf{t}_m^m and \mathbf{u}_m^m are the nodal tractions and displacements vectors on outer matrix boundary, \mathbf{t}_n^m and \mathbf{u}_n^m are the unknown nodal tractions and displacements on the matrix-inclusion interface for the matrix domain.

The unknown parameters in system (5) are the half of the outside boundary discrete values (\mathbf{t}_m^m and \mathbf{u}_m^m) and all discrete values of the inclusion contour \mathbf{t}_n^m and \mathbf{u}_n^m . The additional unknown parameters require extra equations to the linear algebraic system (5). Let us consider the field of the last phase inclusion, denoted as n , isolated from the whole model (Fig. 3(b)). This region consists of two contours again, namely the last inclusion boundary n and the previous phase contour $n-1$. The matrix system of equations carried out for this region with the corresponding elastic properties is:

$$(6) \quad \mathbf{G}^n \cdot \mathbf{t}^n - \mathbf{H}^n \cdot \mathbf{u}^n = \mathbf{0},$$

respectively:

$$(7) \quad \begin{bmatrix} \mathbf{G}_{n,n}^n & \mathbf{G}_{n,n-1}^n \\ \mathbf{G}_{n-1,n}^n & \mathbf{G}_{n-1,n-1}^n \end{bmatrix} \begin{Bmatrix} \mathbf{t}_n^n \\ \mathbf{t}_{n-1}^n \end{Bmatrix} = \begin{bmatrix} \mathbf{H}_{n,n}^n & \mathbf{H}_{n,n-1}^n \\ \mathbf{H}_{n-1,n}^n & \mathbf{H}_{n-1,n-1}^n \end{bmatrix} \begin{Bmatrix} \mathbf{u}_n^n \\ \mathbf{u}_{n-1}^n \end{Bmatrix},$$

$$(7a) \quad \mathbf{t}_n^n = -\mathbf{t}_n^m \quad \text{and} \quad \mathbf{u}_n^n = \mathbf{u}_n^m.$$

Equations (6) must be added to the system (4). Here \mathbf{G}^n and \mathbf{H}^n are global influence matrices for the region n . They could be expressed in extended

form in line with equations (7), where the superscript means the region; the subscript indicates the contour of the source and the field nodal points. Here \mathbf{t}_n^n and \mathbf{u}_n^n are the unknown nodal tractions and the displacements again on the matrix-inclusion interface, but for the last phase inclusion domain. The boundary element discretization of the interface must be in clockwise direction in order to define properly the matrix domain. Conversely, in order to describe correctly the last phase inclusion domain the same interface boundary must be discretized in counter-clockwise direction (Fig. 3(a) and 3(b) – contour n). In that respect, the equilibrium and compatibility conditions of the inclusion-matrix interface are given by equation (7a).

Apparently, all discrete values in system (7) are unknown parameters which cannot be found via the boundary conditions. This fact requires consecutively examination of the rest inclusion phases. Their equations, composed for a single domain with relevant elastic properties, must be added to the previous systems. They are similar to the formula (7). Finally, it could be written for the first inclusion phase (Fig. 4(a)):

$$(8) \quad \mathbf{G}_{1,1}^1 \cdot \mathbf{t}_1^1 - \mathbf{H}_{1,1}^1 \cdot \mathbf{u}_1^1 = \mathbf{0}.$$

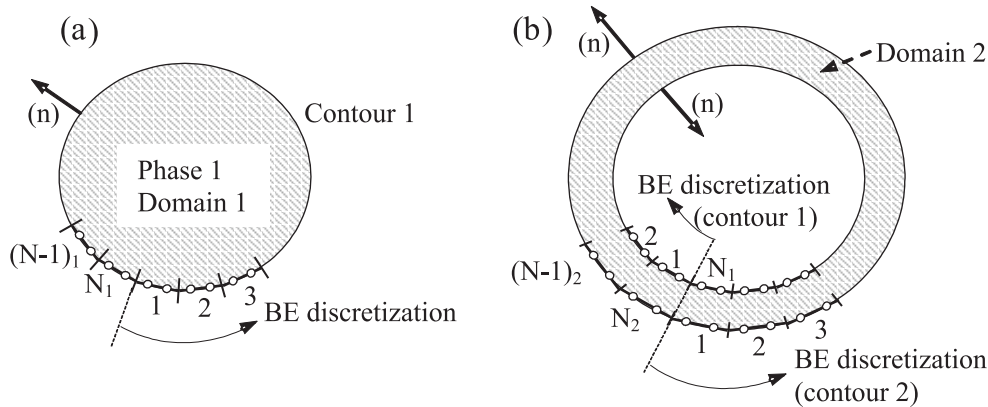


Fig. 4. BE models: (a) first phase of the inclusion; (b) second phase of the inclusion domain

The global system of equations which includes all domains and contours becomes:

$$(9) \quad \begin{bmatrix} \mathbf{G}_{m,m}^m & \mathbf{G}_{m,n}^m & \mathbf{0} & \mathbf{0} & \mathbf{0} & \mathbf{0} & \mathbf{0} & \mathbf{0} \\ \mathbf{G}_{n,m}^m & \mathbf{G}_{n,n}^m & \mathbf{0} & \mathbf{0} & \mathbf{0} & \mathbf{0} & \mathbf{0} & \mathbf{0} \\ \mathbf{0} & \mathbf{G}_{n,n}^n & \mathbf{G}_{n,n-1}^n & \mathbf{0} & \mathbf{0} & \mathbf{0} & \mathbf{0} & \mathbf{0} \\ \mathbf{0} & \mathbf{G}_{n-1,n}^n & \mathbf{G}_{n-1,n-1}^n & \mathbf{0} & \mathbf{0} & \mathbf{0} & \mathbf{0} & \mathbf{0} \\ \mathbf{0} & \mathbf{0} & \mathbf{G}_{n-1,n-1}^{n-1} & \mathbf{G}_{n-1,n-2}^{n-1} & \mathbf{0} & \mathbf{0} & \mathbf{0} & \mathbf{0} \\ \dots & \dots & \dots & \dots & \dots & \dots & \dots & \dots \\ \mathbf{0} & \mathbf{0} & \mathbf{0} & \mathbf{0} & \mathbf{0} & \mathbf{G}_{2,3}^3 & \mathbf{G}_{2,2}^3 & \mathbf{0} \\ \mathbf{0} & \mathbf{0} & \mathbf{0} & \mathbf{0} & \mathbf{0} & \mathbf{0} & \mathbf{G}_{2,2}^2 & \mathbf{G}_{2,1}^2 \\ \mathbf{0} & \mathbf{0} & \mathbf{0} & \mathbf{0} & \mathbf{0} & \mathbf{0} & \mathbf{G}_{1,2}^2 & \mathbf{G}_{1,1}^2 \\ \mathbf{0} & \mathbf{0} & \mathbf{0} & \mathbf{0} & \mathbf{0} & \mathbf{0} & \mathbf{0} & \mathbf{G}_{1,1}^1 \end{bmatrix} \begin{Bmatrix} \mathbf{t}_m \\ \mathbf{t}_n \\ \mathbf{t}_{n-1} \\ \mathbf{t}_{n-2} \\ \dots \\ \mathbf{t}_3 \\ \mathbf{t}_2 \\ \mathbf{t}_1 \end{Bmatrix} = \\
= \begin{bmatrix} \mathbf{H}_{m,m}^m & \mathbf{H}_{m,n}^m & \mathbf{0} & \mathbf{0} & \mathbf{0} & \mathbf{0} & \mathbf{0} & \mathbf{0} \\ \mathbf{H}_{n,m}^m & \mathbf{H}_{n,n}^m & \mathbf{0} & \mathbf{0} & \mathbf{0} & \mathbf{0} & \mathbf{0} & \mathbf{0} \\ \mathbf{0} & \mathbf{H}_{n,n}^n & \mathbf{H}_{n,n-1}^n & \mathbf{0} & \mathbf{0} & \mathbf{0} & \mathbf{0} & \mathbf{0} \\ \mathbf{0} & \mathbf{H}_{n-1,n}^n & \mathbf{H}_{n-1,n-1}^n & \mathbf{0} & \mathbf{0} & \mathbf{0} & \mathbf{0} & \mathbf{0} \\ \mathbf{0} & \mathbf{0} & \mathbf{H}_{n-1,n-1}^{n-1} & \mathbf{H}_{n-1,n-2}^{n-1} & \mathbf{0} & \mathbf{0} & \mathbf{0} & \mathbf{0} \\ \dots & \dots & \dots & \dots & \dots & \dots & \dots & \dots \\ \mathbf{0} & \mathbf{0} & \mathbf{0} & \mathbf{0} & \mathbf{0} & \mathbf{H}_{2,3}^3 & \mathbf{H}_{2,2}^3 & \mathbf{0} \\ \mathbf{0} & \mathbf{0} & \mathbf{0} & \mathbf{0} & \mathbf{0} & \mathbf{0} & \mathbf{H}_{2,2}^2 & \mathbf{H}_{2,1}^2 \\ \mathbf{0} & \mathbf{0} & \mathbf{0} & \mathbf{0} & \mathbf{0} & \mathbf{0} & \mathbf{H}_{1,2}^2 & \mathbf{H}_{1,1}^2 \\ \mathbf{0} & \mathbf{0} & \mathbf{0} & \mathbf{0} & \mathbf{0} & \mathbf{0} & \mathbf{0} & \mathbf{H}_{1,1}^1 \end{bmatrix} \begin{Bmatrix} \mathbf{u}_m \\ \mathbf{u}_n \\ \mathbf{u}_{n-1} \\ \mathbf{u}_{n-2} \\ \dots \\ \mathbf{u}_3 \\ \mathbf{u}_2 \\ \mathbf{u}_1 \end{Bmatrix}$$

The global influence matrices \mathbf{G} and \mathbf{H} , for the whole model (formula (9)), are of block size $(2n + 1) \times (n + 1)$, where n is the number of inclusion phases. The system increases proportionally of the number of inclusions in case of many identical inclusions, as well as the number of the phases. The unknown discrete values are half of the outside boundary parameters, the others are known from the boundary conditions, and all nodal values of the inclusion contours. The final system of linear algebraic equations after satisfying the boundary conditions of the outside contour and rearranging all the known values on the right-hand side and all the unknowns on the left-hand side becomes:

$$(10) \quad \mathbf{A} \cdot \mathbf{x} = \mathbf{B},$$

where \mathbf{x} is the column vector, containing the boundary unknowns, of block dimension $2n + 1$. Matrix \mathbf{A} is the result of the rearrangement of the global influence matrices \mathbf{G} and \mathbf{H} . The size of \mathbf{A} is $(2n + 1) \times (2n + 1)$. \mathbf{B} is a vector of block dimension $2n + 1$ containing the prescribed boundary conditions and the influence matrices of the outside contour.

Obviously, the system of linear algebraic equations is quite large, especially if there are many identical inclusions. In this paper, some new ideas are realized connected to the optimization of the boundary element method which leads to the decreasing the size of the final system of equations. The inclusions are treated similar to openings, independently of the number of different phases. In this case the discretization with boundary elements is only on the last phase inclusion contour, like plain openings, but not stress free.

4. Optimization of the boundary element method for modelling of 2D composite body

The idea of consequently elimination of the inclusion phases will be explained on the example described above. Now the first phase of the inclusion is considered as a single domain (Fig. 4(a)). The matrix system of equations generated for this region is given by formula (8) which can be rearranged as follows:

$$(11) \quad \mathbf{t}_1^1 = (\mathbf{G}_{1,1}^1)^{-1} \cdot \mathbf{H}_{1,1}^1 \cdot \mathbf{u}_1^1.$$

The equilibrium and compatibility conditions on the first phase inclusion contour, respectively at the interface between first and second phases, can be written as:

$$(11a) \quad \mathbf{t}_1^2 = -\mathbf{t}_1^1 \quad \text{and} \quad \mathbf{u}_1^2 = \mathbf{u}_1^1,$$

from where:

$$(11b) \quad \mathbf{t}_1^2 = \mathbf{B}_{1,1} \cdot \mathbf{u}_1^2,$$

$$(12) \quad \mathbf{B}_{1,1} = -(\mathbf{G}_{1,1}^1)^{-1} \cdot \mathbf{H}_{1,1}^1.$$

Matrix $\mathbf{B}_{1,1}$ is a product of the influence matrices $\mathbf{G}_{1,1}^1$ and $\mathbf{H}_{1,1}^1$ generated for the first inclusion phase. This matrix gives the relation between tractions and displacements of the first contour. The displacements are accepted as basic unknowns, while the tractions are expressed by them. So after

the displacements are derived the tractions of the boundary into consideration can be obtained by (11b). It is worthy to note that equations (11), respectively matrix $\mathbf{B}_{1,1}$ are generated for the corresponding contour discretization, namely the mesh for the first domain. The same contour belonging to the second phase possesses different discretization as far as the outside normal is in opposite direction. Therefore the matrix $\mathbf{B}_{1,1}$ must be rearranged properly in accordance with the boundary discretization of the considered domain.

Next, the second phase of inclusion is into consideration as a single discrete model again. The boundary elements mesh and the outside normals are shown in Fig. 4(b). The following system for this domain could be generated:

$$(13) \quad \mathbf{G}^2 \cdot \mathbf{t}^2 - \mathbf{H}^2 \cdot \mathbf{u}^2 = \mathbf{0},$$

or for the tractions of the second domain may be written:

$$(14) \quad \mathbf{t}^2 = (\mathbf{G}^2)^{-1} \cdot \mathbf{H}^2 \cdot \mathbf{u}^2 = \mathbf{C}^2 \cdot \mathbf{u}^2.$$

\mathbf{C}^2 is a matrix similar to $\mathbf{B}_{1,1}$ but a product of the influence matrices \mathbf{G}^2 and \mathbf{H}^2 generated for the second phase region:

$$(15) \quad \mathbf{C}^2 = (\mathbf{G}^2)^{-1} \cdot \mathbf{H}^2.$$

Equations (14) written in an expanded form, in line with the sub- and super- script notations mentioned above, take on the following appearance:

$$(16) \quad \begin{Bmatrix} \mathbf{t}_2^2 \\ \mathbf{t}_1^2 \end{Bmatrix} = \begin{bmatrix} \mathbf{C}_{2,2} & \mathbf{C}_{2,1} \\ \mathbf{C}_{1,2} & \mathbf{C}_{1,1} \end{bmatrix} \cdot \begin{Bmatrix} \mathbf{u}_2^2 \\ \mathbf{u}_1^2 \end{Bmatrix}.$$

By substituting (11b) into (16) we get:

$$(17) \quad \begin{Bmatrix} \mathbf{t}_2^2 \\ \mathbf{B}_{1,1} \cdot \mathbf{u}_1^2 \end{Bmatrix} = \begin{bmatrix} \mathbf{C}_{2,2} & \mathbf{C}_{2,1} \\ \mathbf{C}_{1,2} & \mathbf{C}_{1,1} \end{bmatrix} \cdot \begin{Bmatrix} \mathbf{u}_2^2 \\ \mathbf{u}_1^2 \end{Bmatrix}.$$

The following equation considering the second expression from (17) is derived:

$$(18) \quad \mathbf{u}_1^2 = (\mathbf{B}_{1,1} - \mathbf{C}_{1,1})^{-1} \cdot \mathbf{C}_{1,2} \cdot \mathbf{u}_2^2.$$

By substituting (18) in the first expression (17) the tractions of the second contour are written as:

$$(19) \quad \mathbf{t}_2^2 = \left(\mathbf{C}_{2,2} + \mathbf{C}_{2,1} \cdot (\mathbf{B}_{1,1} - \mathbf{C}_{1,1})^{-1} \cdot \mathbf{C}_{1,2} \right) \cdot \mathbf{u}_2^2.$$

The equilibrium and compatibility conditions in the interface between second and third phases are:

$$(19a) \quad \mathbf{t}_2^3 = -\mathbf{t}_2^2 \quad \text{and} \quad \mathbf{u}_2^3 = \mathbf{u}_2^2,$$

or for the nodal tractions on the second contour for the third domain can be written as follows:

$$(19b) \quad \mathbf{t}_2^3 = \mathbf{B}_{2,2} \cdot \mathbf{u}_2^3, \quad \mathbf{B}_{2,2} = -\left(\mathbf{C}_{2,2} + \mathbf{C}_{2,1} \cdot (\mathbf{B}_{1,1} - \mathbf{C}_{1,1})^{-1} \cdot \mathbf{C}_{1,2}\right).$$

Matrix $\mathbf{B}_{2,2}$ gives the relation between the tractions and the displacements of the second contour. It is a product of the influence matrices \mathbf{G}^2 and \mathbf{H}^2 generated for the second phase region (matrix \mathbf{C}^2) and matrix $\mathbf{B}_{1,1}$ obtained from the previously considered domain.

In such a way, the tractions of any inclusion phase contour i could be expressed by the corresponding displacements. The matrix $\mathbf{B}_{i,i}$ contains the influence matrices of all previous contours. Finally, the last inclusion phase should be considered. The model is shown in Fig. 3(b). The system generated for this region is presented by (6) and (7). For the domain n , following the above derivations, it could be written:

$$(20) \quad \begin{Bmatrix} \mathbf{t}_n^n \\ \mathbf{t}_{n-1}^n \end{Bmatrix} = \begin{Bmatrix} \mathbf{t}_n^n \\ \mathbf{B}_{n-1,n-1} \cdot \mathbf{u}_{n-1}^n \end{Bmatrix} = \begin{bmatrix} \mathbf{C}_{n,n} & \mathbf{C}_{n,n-1} \\ \mathbf{C}_{n-1,n} & \mathbf{C}_{n-1,n-1} \end{bmatrix} \cdot \begin{Bmatrix} \mathbf{u}_n^n \\ \mathbf{u}_{n-1}^n \end{Bmatrix}.$$

Matrix \mathbf{C}^n , given in expanded form in (20), is a product of the influence matrices \mathbf{G}^n and \mathbf{H}^n generated for the n -th phase region. Matrix $\mathbf{B}_{n-1,n-1}$ is derived in the previous step where the phase $n - 1$, with its elastic properties, is taken into account as a single model. The following equations after simple transformations of (20) are reached:

$$(21) \quad \mathbf{u}_{n-1}^n = (\mathbf{B}_{n-1,n-1} - \mathbf{C}_{n-1,n-1})^{-1} \cdot \mathbf{C}_{n-1,n} \cdot \mathbf{u}_n^n.$$

The compatibility and equilibrium conditions in the inclusion-matrix interface are given by equations (7a), from where:

$$(22) \quad \mathbf{t}_n^m = \mathbf{B}_{n,n} \cdot \mathbf{u}_n^m,$$

the matrix $\mathbf{B}_{n,n}$ is denoted as:

$$(23) \quad \mathbf{B}_{n,n} = -\left(\mathbf{C}_{n,n} + \mathbf{C}_{n,n-1} \cdot (\mathbf{B}_{n-1,n-1} - \mathbf{C}_{n-1,n-1})^{-1} \cdot \mathbf{C}_{n-1,n}\right).$$

The tractions of the last inclusion contour expressed by the relevant displacements are given by the formula (22). The equation (23) reflects the influence of all inclusion phases with their mechanical properties and geometrical data. Therefore, the displacements of the last contour could be chosen as basic unknowns, which will be obtained as a solution of the global system of linear algebraic equations, where the boundary conditions of the outside contour are taken into account.

Finally, the matrix domain should be considered. The BE model is shown in Fig. 3(a) and the corresponding system of equations are (4) and (5). By substituting (22) in (5) the following system is derived:

$$(24) \quad \begin{bmatrix} \mathbf{G}_{m,m}^m & \mathbf{G}_{m,n}^m \\ \mathbf{G}_{n,m}^m & \mathbf{G}_{n,n}^m \end{bmatrix} \begin{Bmatrix} \mathbf{t}_m^m \\ \mathbf{B}_{n,n} \mathbf{u}_n^m \end{Bmatrix} = \begin{bmatrix} \mathbf{H}_{m,m}^m & \mathbf{H}_{m,n}^m \\ \mathbf{H}_{n,m}^m & \mathbf{H}_{n,n}^m \end{bmatrix} \begin{Bmatrix} \mathbf{u}_m^m \\ \mathbf{u}_n^m \end{Bmatrix}.$$

The next final system, after simple transformations and regrouping of the contour vectors, is obtained:

$$(25) \quad \begin{bmatrix} \mathbf{G}_{m,m}^m \\ \mathbf{G}_{n,m}^m \end{bmatrix} \{\mathbf{t}_m^m\} = \begin{bmatrix} \mathbf{H}_{m,m}^m & \mathbf{H}_{m,n}^m - \mathbf{G}_{m,n}^m \cdot \mathbf{B}_{n,n} \\ \mathbf{H}_{n,m}^m & \mathbf{H}_{n,n}^m - \mathbf{G}_{n,n}^m \cdot \mathbf{B}_{n,n} \end{bmatrix} \begin{Bmatrix} \mathbf{u}_m^m \\ \mathbf{u}_n^m \end{Bmatrix}.$$

The equations (25) are a type of the usual BE system: $\mathbf{G} \cdot \mathbf{t} = \mathbf{H} \cdot \mathbf{u}$, similar to (9). The influence matrices of the whole model here are \mathbf{G} of block size 2×1 and \mathbf{H} of size 2×2 . Obviously, the dimension of these matrices does not depend on the number of inclusion phases owing to consequently elimination of the internal contours. After satisfying the boundary conditions the unknown parameters are the tractions or displacements of the outside contour and the displacements of the last outer inclusion contour only. Matrix of the right hand side of (25) is the modified influence matrix \mathbf{H} . Apparently, the modification concerns only the components of the influence matrix of the inclusion boundary elements. Once the basic unknowns from (25) are derived the tractions of the external inclusion contour could be obtained by (22). The displacements and tractions of the contour $n-1$ can be derived respectively by (21) and the formula: $\mathbf{t}_{n-1} = \mathbf{B}_{n-1,n-1} \cdot \mathbf{u}_{n-1}$. In a similar, way the discrete values of any contour i can be obtained by:

$$(26) \quad \mathbf{u}_i^{i+1} = (\mathbf{B}_{i,i} - \mathbf{C}_{i,i})^{-1} \cdot \mathbf{C}_{i,i+1} \cdot \mathbf{u}_{i+1}^{i+1},$$

$$(27) \quad \begin{aligned} \mathbf{t}_i^{i+1} &= \mathbf{B}_{i,i} \cdot \mathbf{u}_i^{i+1}, \\ \mathbf{B}_{i,i} &= - \left(\mathbf{C}_{i,i} + \mathbf{C}_{i,i-1} \cdot (\mathbf{B}_{i-1,i-1} - \mathbf{C}_{i-1,i-1})^{-1} \cdot \mathbf{C}_{i-1,i} \right). \end{aligned}$$

A software program based on the dual boundary element method has been previously developed by the author, using Visual Basic for Application (VBA) in Excel environment [9]. In that work, a discontinuous double-node linear boundary element has been developed in order to solve linear and non-linear plane elasticity crack problems. In the present study, the same program is used to which an upgrading and adjustment is made for the modelling of the composite medium.

5. Numerical example

The presented numerical example is a static solution of a square plate with a single inclusion of two phases (Fig. 5). The aim of this numerical model is to compare the results obtained by the application of the presented procedure against the results developed by using Finite Element Method (FEM) and general purpose software packages. The inclusion is a fiber one with a coating layer. The radius of the fiber is 0.1 and the thickness of the inter-phase is 0.2. The coating layer is inhomogeneous with constant Poisson ratio and varying modulus of elasticity. The Young's modulus of the fiber is 10, the modulus of the matrix is 1, the protecting coating has linear elastic modulus variation between the ones of the fiber and the matrix. The loading and boundary conditions are assumed similar to these used for the modelling of the unit cell from a multi phase inclusions composite presented in Fig. 1. The geometrical and mechanical properties of the example along with the loading and boundary conditions are given in Fig. 5. Young's modulus with linear variation along the radius direction is given on the right. The inter-phase is divided into five rings in order to take into account the variation of the inter-phase properties. The elastic modulus of each "ring like" portion is assumed constant equal to arithmetical mean and subsequently, the presented procedure is applied.

In what follows, two numerical models are presented. The boundary elements model consists of six inclusion contours. The outside boundary contains 80 boundary elements and each inclusion contour has been modelled by 56 boundary elements. The final numerical model, which consists of 136 boundary elements and respectively twice more nodes (Fig. 6(a)), is obtained after consecutively exclusion of the interior inclusion domains with application of the presented procedure and BEM. A parallel solution by FEM and ANSYS software program has been performed. An isoparametric finite element for plane elasticity problems PLANE 42 is used in this model with two nodal degrees of freedom. Very fine finite element mesh has been employed in order to obtain more accurate results. This mesh consists of 24679 finite elements and 24875 nodes and the corresponding model is given in Fig. 6(b).

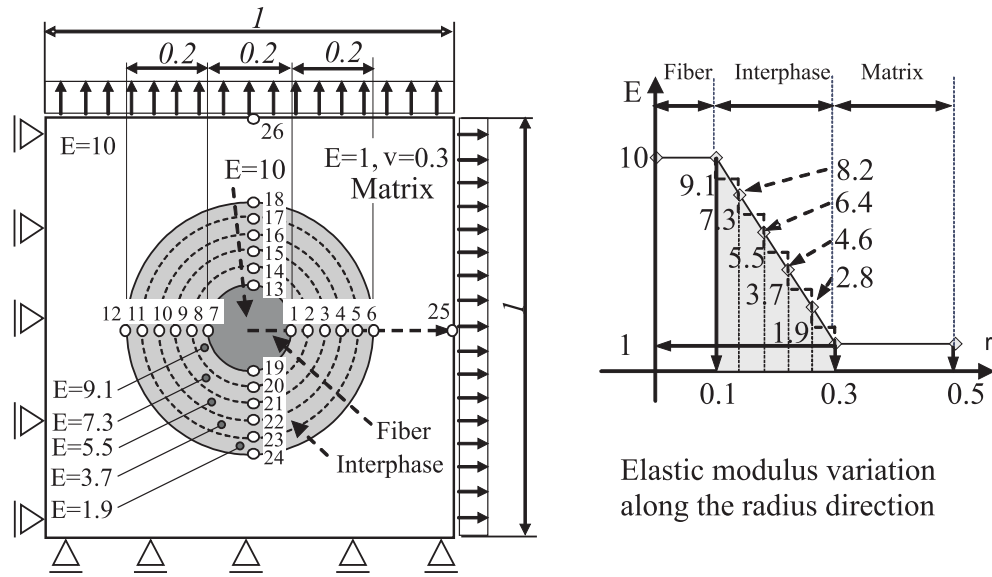


Fig. 5. Numerical example: geometrical, material data, loading and boundary supports

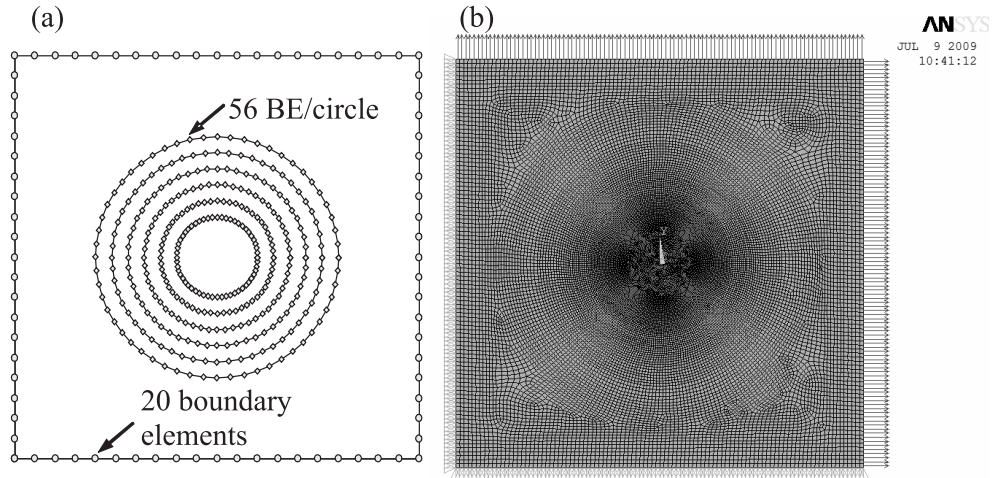


Fig. 6. Numerical models: (a) BEM model, (b) FEM model

Present modelling

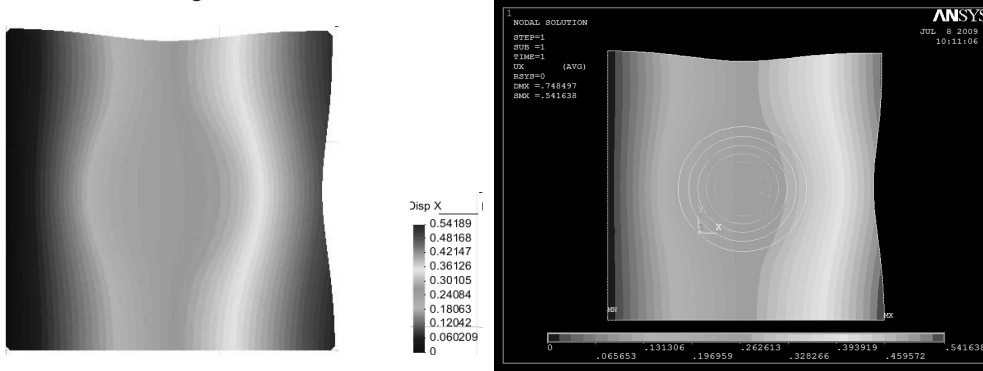


Fig. 7. Horizontal displacements in X direction

Table 1

point		Stresses σ_x		diffe- rence %	point		Stresses σ_x		diffe- rence %
		BEM	FEM				BEM	FEM	
1		1.482	1.482	0.00	17	$E = 3.7$	0.9547	0.9527	0.21
2		1.451	1.452	0.07		$E = 1.9$	0.7373	0.7322	0.69
3		1.397	1.399	0.14	18	$E = 1.9$	0.8037	0.8008	0.36
4		1.332	1.336	0.30		$E = 1$	0.5518	0.5478	0.73
5		1.26	1.265	0.40	19	$E = 10$	1.505	1.504	0.07
6		1.188	1.185	0.25		$E = 9.1$	1.41	1.409	0.07
7		1.514	1.514	0.00	20	$E = 9.1$	1.436	1.434	0.14
8		1.496	1.493	0.20		$E = 7.3$	1.241	1.238	0.24
9		1.453	1.449	0.28	21	$E = 7.3$	1.288	1.286	0.16
10		1.399	1.395	0.29		$E = 5.5$	1.078	1.074	0.37
11		1.337	1.331	0.45	22	$E = 5.5$	1.134	1.131	0.26
12		1.273	1.266	0.55		$E = 3.7$	0.9009	0.897	0.43
13	$E = 10$	1.498	1.497	0.07	23	$E = 3.7$	0.9613	0.9591	0.23
	$E = 9.1$	1.404	1.402	0.14		$E = 1.9$	0.7499	0.745	0.66
14	$E = 9.1$	1.427	1.425	0.14	24	$E = 1.9$	0.8104	0.807	0.42
	$E = 7.3$	1.232	1.228	0.33		$E = 1$	0.5689	0.5658	0.55
15	$E = 7.3$	1.28	1.278	0.16	25	1	0.9992	0.08	
	$E = 5.5$	1.068	1.063	0.47	26	0.6248	0.6165	1.34	
16	$E = 5.5$	1.126	1.124	0.18					
	$E = 3.7$	0.8894	0.8848	0.52					

The deformed shapes with the corresponding colour diagrams of horizontal displacements are given in Fig. 7. The graphics cannot be absolutely the same because the colour intensity scales are different, but a comparison between representative points of both models shows a very good agreement with the numerical values. It could be seen from the diagrams that the difference in the extreme values of the horizontal displacements is 0.05%.

The stress intensity diagrams in the X direction, obtained by both models, are presented in Fig. 8. The stresses in Y direction are the same because of the diagonal symmetry of the example respectively the diagram is the same but in vertical direction. A comparison for the stress values for the representative points, plotted in Fig. 5, obtained by present and FEM solutions is given in table 1.

It should be pointed out that the stresses of the boundary nodes between two regions with different modulus of elasticity are different depending on which domain are extracted. That could be seen in Fig. 7 and Fig. 8 the displacements on the boundaries between “ring like” portions of the inter-phase are equal, but there is a jump in the stresses corresponding to the jump in the Young’s modulus.

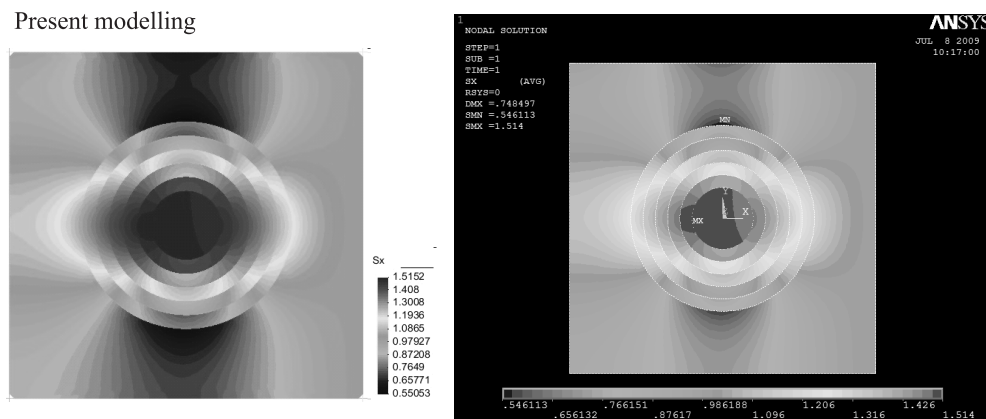


Fig. 8. Stress intensity diagrams in X direction

6. Conclusion

It could be concluded based on the above numerical example and comparison of the results that the presented procedure for consecutively exclusion of the unknown contour values of multi phase inclusions works with higher accuracy as compared to FEM solutions. This procedure is very suitable for

modelling of the composite bodies with large number of identical inclusions because its application results to considerable reduction of the model degrees of freedom respectively the computational time. The reduction is proportional to the number of inclusion phases, larger number of phases smaller degrees of freedom compared to classical BEM modelling. Once the basic unknowns, namely unknown boundary values of the outside contour and displacements of the last inclusion contour, are derived the discrete values of the other boundaries are obtained by consecutive application of equations (26) and (27).

The presented optimization is applicable for the case of coating inter-phase with variable elastic properties if the division to "ring like" portion is possible. Usually, the inter-phases are small in thickness and it should be pointed out that if each "ring like" domain (Fig. 6(a)) has a thickness smaller than the length of the corresponding boundary elements the accuracy of BEM solution is questionable. In this case an appropriate optimization technique should be employed, which will be the objective of future work.

REFERENCES

- [1] GROSS, D., T. SEELIG. Fracture Mechanics with an Introduction to Micromechanics, Berlin, Springer-Verlag, Heidelberg, 2006.
- [2] DRAGO, A., M. PINDERA. Micro-macromechanical Analysis of Heterogeneous Materials: Macroscopically Homogeneous vs Periodic Microstructures. *Composites Science and Technology*, **67** (2007), 1243–1263.
- [3] WACKER, G., A. BLEDZKI, A. CHATE. Effect of Interphase on the Trasverse Young's Modulus of Glass/epoxy Composites. *Composites Part A*, **29A** (1998), 619–626.
- [4] DONG, Y. Effective Elastic Properties of Doubly Periodic Array of Inclusions of Various Shapes by the Boundary Element Method. *International Journal of Solids and Structures*, **43** (2002), 7919–7938.
- [5] WANG, J., S. CROUCH, S. MOGILEVSKAYA. Numerical Modelling of the Elastic Behavior of Fiber-reinforced Composites with Inhomogeneous Interphases. *Composites Science and Technology*, **66** (2006), 1–18.
- [6] YAO, Z., F. KONG, H. WANG, P. WANG. 2D Simulation of Composite Materials using BEM. *Engineering Analysis with Boundary Elements*, **28** (2004), 927–935.
- [7] CHEN, X., YIJUN LIU. Multiple-cell Modelling of Fiber-reinforced Composites with the Presence of Interphases using the Boundary Element Method. *Computational Materials Science*, **21** (2001), 86–94.

- [8] BREBBIA, C., J. TELLES, L. WROBEL. Boundary Element Techniques: Theory and Applications in Engineering, Moscow, Mir, 1987 (in Russian – translation from English).
- [9] PARVANOVA, S. Dual Boundary Element Method, Annual of UACEG, Sofia, Vol. **XLII**, 2005–2006 (in Bulgarian).